Journal of Zhejiang University-SCIENCE A (Applied Physics & Engineering)
ISSN 1673-565X (Print); ISSN 1862-1775 (Online)
www.zju.edu.cn/jzus; www.springerlink.com
E-mail: jzus@zju.edu.cn

Experiments and sensitivity analyses for heat transfer in a meter-scale regularly fractured granite model with water flow*

Wei LU[1,2], Yan-yong XIANG[†‡1]

([1]*School of Civil Engineering, Beijing Jiaotong University, Beijing 100044, China*)

([2]*State Key Laboratory of Simulation and Regulation of Water Cycle in River Basin, China Institute of Water Resources and Hydropower Research, Beijing 100038, China*)

[†]E-mail: xiang_yanyong@263.net

Received July 20, 2012; Revision accepted Oct. 26, 2012; Crosschecked Nov. 19, 2012

Abstract: Experiments of saturated water flow and heat transfer were conducted for a meter-scale model of regularly fractured granite. The fractured rock model (height 1502.5 mm, width 904 mm, and thickness 300 mm), embedded with two vertical and two horizontal fractures of pre-set apertures, was constructed using 18 pieces of intact granite. The granite was taken from a site currently being investigated for a high-level nuclear waste repository in China. The experiments involved different heat source temperatures and vertical water fluxes in the embedded fractures either open or filled with sand. A finite difference scheme and computer code for calculation of water flow and heat transfer in regularly fractured rocks was developed, verified against both the experimental data and calculations from the TOUGH2 code, and employed for parametric sensitivity analyses. The experiments revealed that, among other things, the temperature distribution was influenced by water flow in the fractures, especially the water flow in the vertical fracture adjacent to the heat source, and that the heat conduction between the neighboring rock blocks in the model with sand-filled fractures was enhanced by the sand, with larger range of influence of the heat source and longer time for approaching asymptotic steady-state than those of the model with open fractures. The temperatures from the experiments were in general slightly smaller than those from the numerical calculations, probably due to the fact that a certain amount of outward heat transfer at the model perimeter was unavoidable in the experiments. The parametric sensitivity analyses indicated that the temperature distribution was highly sensitive to water flow in the fractures, and the water temperature in the vertical fracture adjacent to the heat source was rather insensitive to water flow in other fractures.

Key words: Fractured granite, Water flow, Heat transfer, Physical modeling, Numerical calculation, Sensitivity analysis
doi:10.1631/jzus.A1200153 **Document code:** A **CLC number:** X141

1 Introduction

Underground disposal of high-level nuclear waste induces coupled thermal, hydrological, mechanical, and chemical (THMC) processes in the geological barrier, especially in the near field of waste repositories. Theoretical and numerical calculations, laboratory experiments, and large scale field investigations have contributed to establishing better knowledge of the coupling phenomena in a suit of potential host rocks for containing, retarding, and diluting radionuclides leaked out of the engineering barrier over hundreds of thousands of years after the disposal. Various types of rocks, including clay, salt, granite, and tuff, have been selected for investigation. The Beishan area in the Gansu province of China has been studied as a potential site for high level nuclear waste disposal in the country. According to preliminary surface mapping investigations, the site is composed of large saturated granite bodies with average fracture spacing on the order of meters, and the fractures are largely open with 78% of apertures in the range of 1 to 3 mm, 12% in the range of 3 to 5 mm, and less than 5% larger than 10 mm. The radioactive

‡ Corresponding author

* Project (No. 50778014) supported by the National Natural Science Foundation of China

heat of nuclear waste would influence the performance of the granite mass as a natural barrier to the migration of radionuclides to the accessible environment. For understanding and evaluating various relevant coupling processes, and for aiding the repository layout design and waste-package thermal loading design, it is necessary to study the characteristics of convective and conductive heat transfer in the fractured granite mass.

Considering single-fracture water-flow induced heat advection and the perpendicular 1D heat conduction in an infinite rock matrix, some analytical solutions are presented by Gringarten *et al*. (1975), Čermak and Jetel (1985), and Schulz (1987). Taking into account 2D and 3D heat conductions in rock matrix, semi-analytical formulations are developed by Cheng *et al*. (2001) and Ghassemi *et al*. (2003), respectively. Xiang and Guo (2011) and Xiang and Zhang (2012) extended the formulation of Cheng *et al*. (2001) to consider distributed heat sources and heat advections by water-flow in multiple fractures.

Research on the THM behavior of the host rock of a nuclear waste repository has been done under the international collaboration project of Development of Coupled Models and Their Validation Against Experiment in Nuclear Waste Isolation (DECOVALEX) begun in 1992 (Jing *et al*. 1995; Tsang *et al*., 2005; Tsang *et al*., 2009). The project has undergone four stages, and progress has been made in several areas, such as bench mark test (Chan *et al*., 1995; Millard *et al*., 1996; Wilcock, 1996), numerical simulations of long term near field and far field THM behaviors (Rutqvist *et al*., 2005; Liu *et al*., 2006), underground heater test, and validation of numerical simulations (Chijimatsu *et al*., 2001; Rutqvist *et al*., 2001; Alonso *et al*., 2005), and incorporation of chemical effects (Ito *et al*., 2004).

In the present study, granite taken from the Beishan area in Gansu province was cut, trimmed, and then assembled into a fractured rock model of 1502.5 mm in height, 904 mm in width, and 300 mm in thickness, composed of nine rock blocks with two vertical and two horizontal fractures. An electric heating plate was placed on one side of the fractured rock model, and temperature sensors and pressure sensors were installed in the interior. Water flow and heat transfer experiments were conducted under open and sand-filled conditions, respectively. Numerical calculations using both a self-developed finite difference scheme and the TOUGH2 code were carried out to compare with experimental data, and the influences of the major model parameters, including heat source temperature and water velocities of the vertical fractures, on the outflow water temperatures of the model were analyzed.

2 Experimental model setup and schemes

As shown in Fig. 1, the model system setup was composed of the following five parts:

1. Fractured rock model: Using granite from a potential site for hosting the high level nuclear waste repository in China, a fractured rock model of height 1502.5 mm, width 904 mm, and thickness 300 mm was assembled with nine rock blocks, which formed, with miniaturised steel spacers in between, two vertical fractures, V_1 of aperture 1.5 mm and V_2 of aperture 2.5 mm, and two horizontal fractures, H_1 of aperture 1.5 mm and H_2 of aperture 1.0 mm. Values of physical parameters of the rock matrix samples were determined through laboratory measurements, as shown in Table 1 for two different ambient temperatures.

2. Water flow: Water flow into the two vertical fractures was maintained by two constant-flow pumps at the top ends of the fractures and recorded by two glass rotor flow meters at the bottom ends of the fractures.

3. Heat source: An electric heating plate with a height of 1500 mm, width of 300 mm, and thickness of 3 mm was placed on one side of the fractured rock model as the heat source, with its temperature pre-set and maintained by a temperature controller with an accuracy of 1%.

4. Insulation of heat: Heat insulation was realized by attaching waterproof rock-wool boards, with a thickness of 100 mm and a low thermal conductivity of $(0.027+0.00017T)$ W/(m·°C) (T, temperature in °C), to all six interior surfaces of a stainless steel model box.

5. Data acquisition: 42 thermal resistance temperature sensors, 35 mm in length, and 3 mm in diameter with a measurement accuracy of $\pm(0.15+0.002T)$ °C in the range of −50 to 250 °C, were embedded in both the interiors of the rock blocks and the interfaces with the fractures. A total of 12 fluid

pressure sensors, 15 mm in length and 3.8 mm in diameter with a measurement accuracy of ±0.003p kPa (p, fluid pressure in kPa) in the range of 0 to 400 kPa at temperatures from 0 to 100 °C, were placed within the fractures. During the experimental processes, a multi-channel data acquisition instrument with an extension module was employed to record every 30 s the temperatures of the sensors with ±0.1 °C accuracy and the pressures of the pressure sensors with ±0.1 kPa accuracy.

As shown in Table 2, three groups of experiments were carried out. The two experiments of group 1 varied heat source temperature with constant water flux in the two vertical open fractures. The two experiments of group 2 varied water flux in the two vertical open fractures with a constant heat source temperature. The two experiments of group 3 had a constant heat source temperature and a constant water flux in the two vertical fractures when filled with sand of diameters from 0.50 to 0.63 mm.

Table 1 Parameters values of the granite for two different ambient temperatures

Ambient temperature (°C)	Density (g/cm^3)	Specific heat (J/(g·°C))	Thermal diffusion coefficient (mm^2/s)	Thermal conductivity (W/(m·°C))
25	2.70	0.686	1.244	2.30
125	2.70	0.812	1.013	2.22

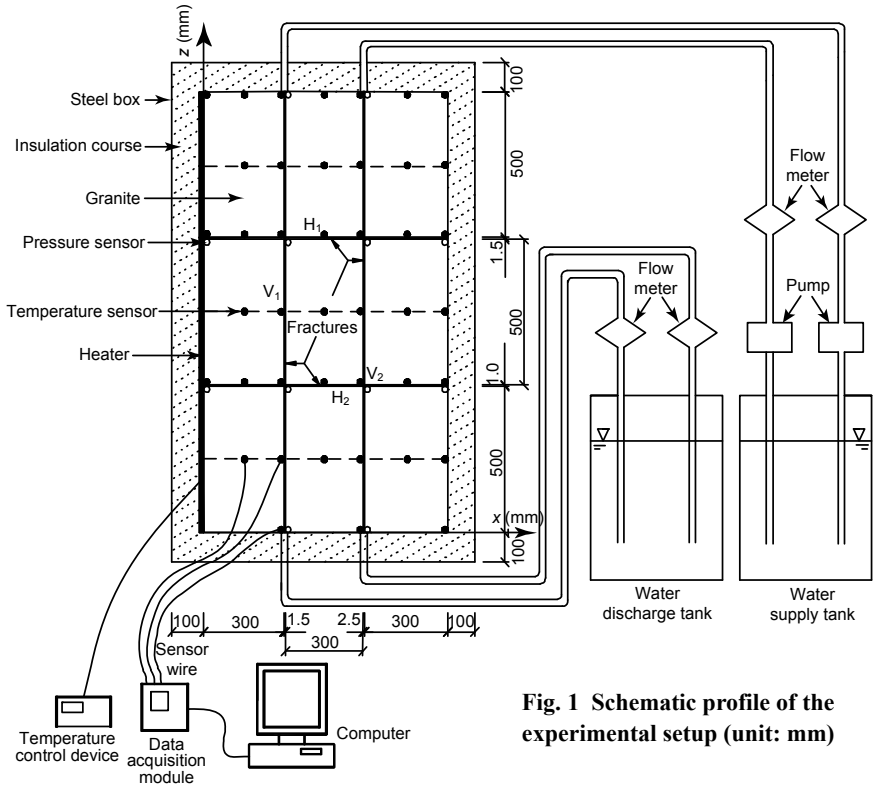

Fig. 1 Schematic profile of the experimental setup (unit: mm)

Table 2 Experimental schemes

Serial of experiment		Vertical fracture porosity	Heat source temperature (°C)	Inflow water temperature (°C)	Water velocity in vertical fracture (mm/s)	
					Fracture V_1	Fracture V_2
Group 1	a	1	70	15.5	2.5	5.0
	b	1	95	15.5	2.5	5.0
Group 2	c	1	95	16.2	5.0	5.0
	d	1	95	15.9	2.5	2.5
Group 3	e	0.55	95	16.4	2.2	2.4
	f	0.55	120	16.4	2.2	2.4

The temperature of the inflow water was variable due to fluctuations of the ambient temperature in the laboratory. Three different heat source temperatures (70, 95, and 120 °C) were employed in the experiments.

3 Observations based on experimental data

As shown in Fig. 2 for the water temperatures at the outlets of the two vertical fractures, the heat advection of water flow and the heat conduction between the rock blocks induced four stages of temperature variations in the model system, from initial gradual increase and intermediate quick increase to later slow increase and final quasi steady state, in all six experimental schemes.

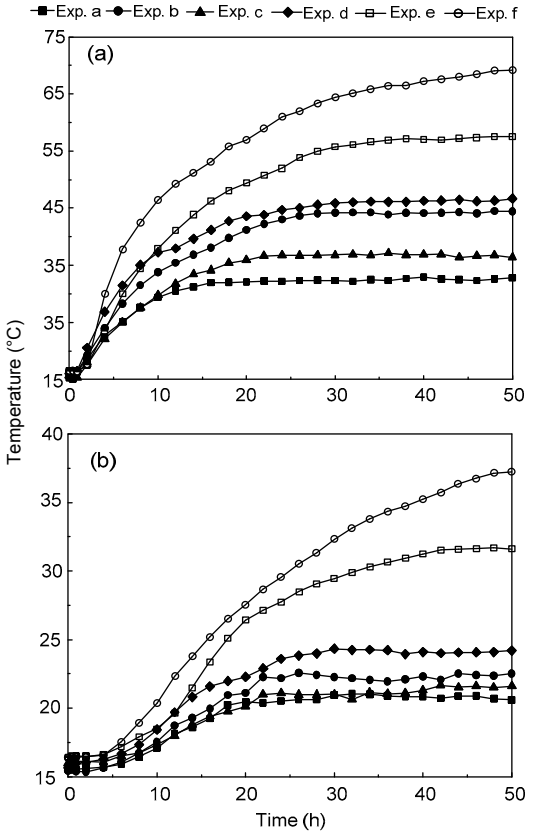

Fig. 2 Temporal variations of outflow water temperatures of fracture V_1 (a) and fracture V_2 (b)

Fig. 3 shows distributions of the steady state temperature in the fractured rock model for the six experimental schemes in Table 2.

Based on the experimental data, the following observations can be made:

1. Heat advection due to water flow in the vertical fractures took a certain percentage of the input thermal energy out of the model and impeded heat conduction in the transverse direction. Such an effect was the most prominent for fracture V_1 due to its closeness to the heat source (Fig. 3a), while the maximum increase of temperature of the model periphery on the far side away from the heat source was only 0.5 °C for experiment a.

2. Such thermal energy depravation and impedance effects due to heat advection increased as the water flux in the fractures increased, and decreased as the heat source temperature and/or the distance of the fracture away from the heat source increased, as can be seen through comparisons between Figs. 3b, 3c, and 3d.

3. Comparing Figs. 3e and 3f with Figs. 3d, one may see that due to the enhanced heat conduction when the fractures were filled with sand, transverse heat transfer became more pronounced than the cases with open fractures.

4. Water in the two horizontal fractures remained standstill and thus mainly played a role of heat storage and conduction in the experimental processes, and under the experimental conditions the volumetric specific heat of water is about twice as large as that of the granite while the thermal conductivity of water is about 27% of that of the granite.

5. There was no phase change of the water in the fractures, even when the temperature of water in the fracture most adjacent to the heater exceeded 100 °C. This phenomenon was not considered as an abnormality of the experiment, because the system was essentially a closed system without direct exposure of the fractured rock model to the atmosphere, in addition, the fractured rock model was only permeable in the fractures and the percentage of the water with temperatures exceeding 100 °C was relatively small. The hydraulic head at steady state assumed nearly linear distribution along the vertical fractures (Fig. 4).

4 Mathematical model and numerical scheme

4.1 Governing equations

Neglect the permeability and water storage of the granite blocks, and assume constant temperature across the apertures of the fractures. Within the

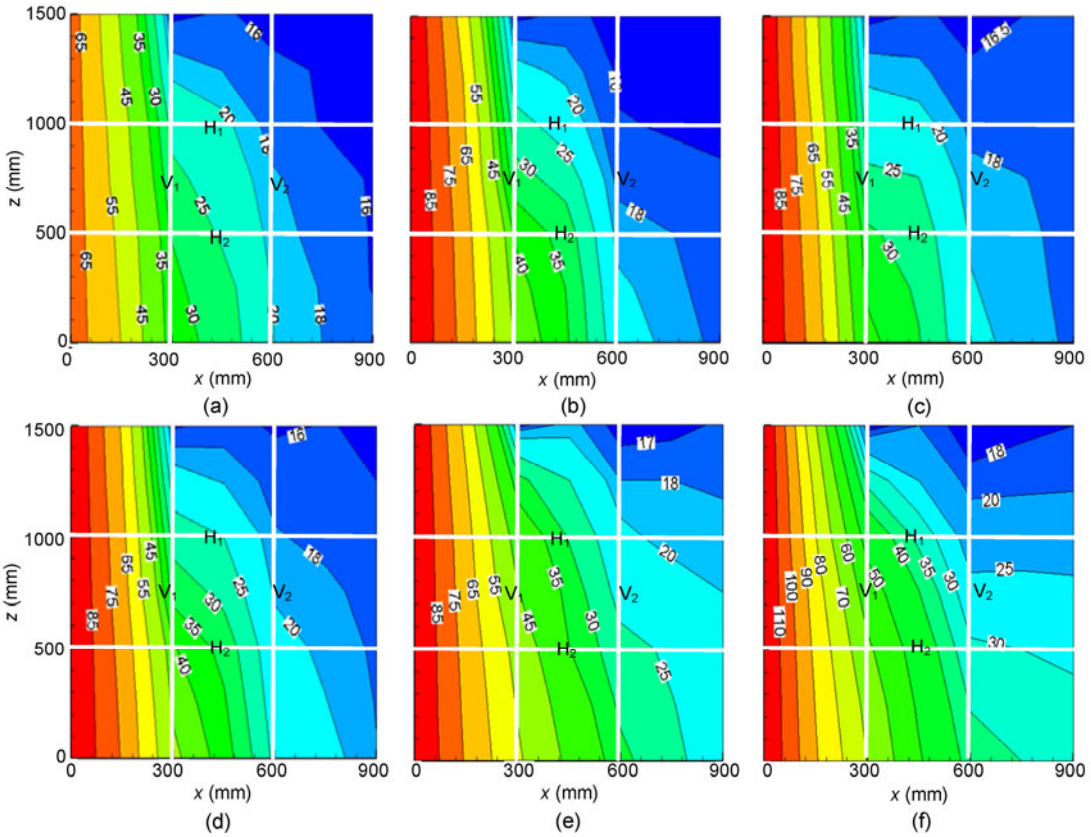

Fig. 3 Temperature field of the fractured rock model at steady state for different experiments (unit: °C)
(a)–(f) are experiments a–f, respectively

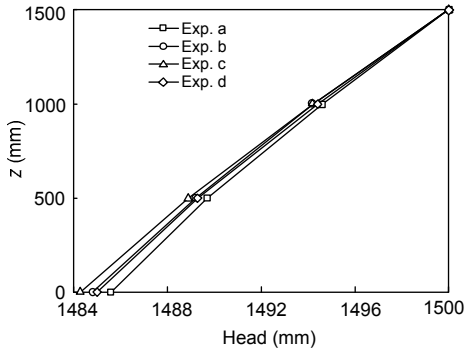

Fig. 4 Hydraulic head in vertical fractures at steady state

vertical fractures, since heat transfer is dominated by advection, the thermal diffusion and dispersion effects are comparatively small and assumed to be negligible. Referring to the *x*-*z* system of coordinates shown in Fig. 1, the thermal energy conservation equation can be written as

$$\frac{\partial(e\rho_{\mathrm{m}}c_{\mathrm{m}}T_{\mathrm{w}})}{\partial t}+\frac{\partial(\phi ve\rho_{\mathrm{w}}c_{\mathrm{w}}T_{\mathrm{w}})}{\partial z}-K_{\mathrm{r}}\left(\left.\frac{\partial T_{\mathrm{r}}}{\partial x}\right|_{x=e^{-}}-\left.\frac{\partial T_{\mathrm{r}}}{\partial x}\right|_{x=e^{+}}\right)=0, \tag{1}$$

where v is the water velocity in the fracture; e is the aperture of the fracture; T_{w}, ρ_{w}, and c_{w} are the temperature, density, and specific heat of water, respectively; ϕ, ρ_{s}, and c_{s} are the porosity, density, and specific heat of the filling material within the fractures, respectively; T_{r} and K_{r} are the temperature and the thermal conductivity of the rock matrix, respectively; $\left.\frac{\partial T_{\mathrm{r}}}{\partial x}\right|_{x=e^{-}}$ and $\left.\frac{\partial T_{\mathrm{r}}}{\partial x}\right|_{x=e^{+}}$ are the derivatives evaluated at the left and right walls of the vertical fractures, respectively; $\rho_{\mathrm{m}}c_{\mathrm{m}}$ is the composite volumetric specific heat of the fill and water in the fracture and $\rho_{\mathrm{m}}c_{\mathrm{m}}=\phi\rho_{\mathrm{w}}c_{\mathrm{w}}+(1-\phi)\rho_{\mathrm{s}}c_{\mathrm{s}}$.

The governing equation for heat transfer in the horizontal fractures without water flow is

$$\frac{\partial(e\rho_{\mathrm{w}}c_{\mathrm{w}}T_{\mathrm{w}})}{\partial t}-eK_{\mathrm{w}}\frac{\partial^{2}T_{\mathrm{w}}}{\partial x^{2}}-K_{\mathrm{r}}\left(\left.\frac{\partial T_{\mathrm{r}}}{\partial z}\right|_{z=e^{-}}-\left.\frac{\partial T_{\mathrm{r}}}{\partial z}\right|_{z=e^{+}}\right)=0, \tag{2}$$

where K_{w} denotes the thermal conductivity of water,

and $\left.\frac{\partial T_\mathrm{r}}{\partial z}\right|_{z=e^-}$ and $\left.\frac{\partial T_\mathrm{r}}{\partial z}\right|_{z=e^+}$ are the derivatives evaluated at the lower and upper walls of the horizontal fractures, respectively.

The governing equation for heat transfer in the rock matrix is

$$\frac{\partial(\rho_\mathrm{r} c_\mathrm{r} T_\mathrm{r})}{\partial t} - K_\mathrm{r}\left(\frac{\partial^2 T_\mathrm{r}}{\partial x^2} + \frac{\partial^2 T_\mathrm{r}}{\partial z^2}\right) = 0. \tag{3}$$

Let T represent T_r or T_w, then the initial condition, the heat source boundary condition, the water inlet boundary condition, and the approximated adiabatic boundary conditions can be written as

$$\begin{cases} T\big|_{t=0} = T_0, \\ T\big|_{x=0} = T_\mathrm{h}, \\ T\big|_{x=300\,\mathrm{mm},\, z=1500\,\mathrm{mm}} = T_0, \\ T\big|_{x=600\,\mathrm{mm},\, z=1500\,\mathrm{mm}} = T_0, \\ \left.\frac{\partial T}{\partial z}\right|_{z=0} = \left.\frac{\partial T}{\partial z}\right|_{z=1500\,\mathrm{mm}} = 0, \\ \left.\frac{\partial T}{\partial x}\right|_{x=900\,\mathrm{mm}} = 0, \end{cases} \tag{4}$$

where T_0 denotes the initial temperature and T_h denotes the heat source temperature. Note that the front and rear boundaries of the model were also kept insulated in the experiments, but the relevant boundary conditions are not needed here for heat transfer in the x-z plane, because there was no thermal gradient in the thickness direction.

4.2 Finite difference scheme

Referring to Fig. 5, the finite difference forms of Eqs. (1)–(4) can be expressed, respectively, as

$$\frac{\partial T_{ij}}{\partial t} = \frac{1}{\rho_\mathrm{m} c_\mathrm{m}} \times \left(K_\mathrm{r} \frac{T_{i,j-1} - 2T_{ij} + T_{i,j+1}}{e\Delta x} + v\phi\rho_\mathrm{w} c_\mathrm{w} \frac{T_{i-1,j} - T_{i+1,j}}{2\Delta z} \right), \tag{5}$$

$$\frac{\partial T_{ij}}{\partial t} = \frac{1}{\rho_\mathrm{w} c_\mathrm{w}} \times \left(K_\mathrm{r} \frac{T_{i-1,j} + T_{i+1,j}}{e\Delta z} + K_\mathrm{w} \frac{T_{i,j-1} + T_{i,j+1}}{(\Delta x)^2} - 2\left(\frac{K_\mathrm{r}}{e\Delta z} + \frac{K_\mathrm{w}}{(\Delta x)^2}\right) T_{ij} \right), \tag{6}$$

$$\frac{\partial T_{ij}}{\partial t} = \frac{K_\mathrm{r}}{\rho_\mathrm{r} c_\mathrm{r}} \times \left(\frac{T_{i,j+1} + T_{i,j-1}}{(\Delta x)^2} + \frac{T_{i+1,j} + T_{i-1,j}}{(\Delta z)^2} - 2\left(\frac{1}{(\Delta x)^2} + \frac{1}{(\Delta z)^2}\right) T_{ij} \right), \tag{7}$$

$$\begin{cases} T_{ij}\big|_{t=0} = T_0, \\ T_{ij}\big|_{x_j=0} = T_\mathrm{h}, \\ T_{ij}\big|_{x_j=300\,\mathrm{mm},\, z_i=1500\,\mathrm{mm}} = T_0, \\ T_{ij}\big|_{x_j=600\,\mathrm{mm},\, z_i=1500\,\mathrm{mm}} = T_0, \\ \left.\frac{T_{i+1,j} - T_{i-1,j}}{2\Delta z}\right|_{z_i=0,\,1500\,\mathrm{mm}} = 0, \\ \left.\frac{T_{i,j+1} - T_{i,j-1}}{2\Delta x}\right|_{x_j=900\,\mathrm{mm}} = 0, \end{cases} \tag{8}$$

where T_{ij} stands for the temperature of grid point (x_j, z_i) at time t, and the subscripts w and r are for water and rock temperatures, respectively, have been omitted for brevity.

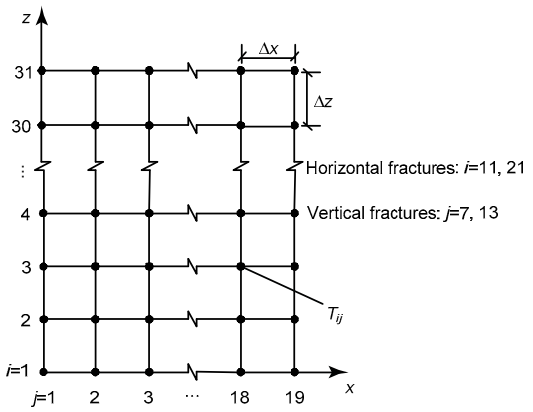

Fig. 5 Finite difference grid of the fractured rock model (Δx=Δz=50 mm)

Eqs. (5)–(7) can all be expressed as

$$\frac{\partial T_{ij}}{\partial t} = f(T_{ij}), \tag{9}$$

where $f(T_{ij})$ stands for the right hand side of any of Eqs. (5)–(7). Equations in the form of Eq. (9) can be solved using the 4th order Runge-Kutta integration scheme based on the 1/3 Simpson's rule:

$$\begin{cases} k_1 = f(T_{ij}^n), \\ k_2 = f\left(T_{ij}^n + \dfrac{1}{2}k_1\Delta t\right), \\ k_3 = f\left(T_{ij}^n + \dfrac{1}{2}k_2\Delta t\right), \\ k_4 = f(T_{ij}^n + k_3\Delta t), \\ T_{ij}^{n+1} = T_{ij}^n + \dfrac{\Delta t}{6}(k_1 + 2k_2 + 2k_3 + k_4), \end{cases}$$

where Δt denotes the time step and T_{ij}^n denotes the temperature of grid point (x_j, z_i) at time $t^n=n\Delta t$, n=0, 1, 2, ⋯.

According to Tao (2003), for the above explicit procedure to be applicable to Eqs. (5)–(7), the stability conditions that the spatial and temporal divisions must satisfy can be expressed as

$$\begin{cases} 0 \le \dfrac{4K_{\mathrm{m}}\Delta t}{\rho_{\mathrm{m}}c_{\mathrm{m}}(\Delta x)^2} \le 1, \\ 0 \le \dfrac{(v/e)^2\left(\rho_{\mathrm{m}}c_{\mathrm{m}}(\Delta x)^2\right)\Delta t}{2K_{\mathrm{m}}} \le 1, \end{cases} \tag{10a}$$

$$0 \le \frac{2K_{\mathrm{w}}\Delta t}{\rho_{\mathrm{w}}c_{\mathrm{w}}e^2} + \frac{2K_{\mathrm{r}}\Delta t}{\rho_{\mathrm{r}}c_{\mathrm{r}}(\Delta x)^2} \le 1, \tag{10b}$$

$$0 \le \frac{4K_{\mathrm{r}}\Delta t}{\rho_{\mathrm{r}}c_{\mathrm{r}}(\Delta x)^2} \le 1. \tag{10c}$$

5 Comparisons between numerical results and experimental data

Using the parameter values in Table 3, numerical calculations were carried out by using both the above numerical scheme and the TOUGH2 software. The EOS3 module of TOUGH2 was employed through an effective continua approach with a prescribed level of near full saturation for the fracture continuum elements, as described by Liu and Xiang (2012). The numerical results in comparison with the experimental data are presented in terms of the surplus temperature relative to the initial temperature, as shown in Figs. 6 and 7 for experiment b, and in Figs. 8 and 9 for experiment e.

For temporal variations of the temperature of the outflow water in the vertical fractures, one may see from Figs. 6 and 8 that there is generally good consistency between the numerical calculations and the experimental data, and that when approaching steady state the experimental data become smaller than the numerically calculated values. The effects due to some degree of unavoidable heat loss during the experiments, though relatively minor in general, can get more pronounced at locations further away from the heat source where the temperatures are significantly lower than the heat source temperature, as depicted in Figs. 7 and 9.

Table 3 Averaged parameter values for the numerical calculations

Material	Density (g/cm^3)	Specific heat (J/(g·°C))	Thermal conductivity (W/(m·°C))
Water	1.00	4.18	0.60
Granite	2.70	0.75	2.26
Sand	2.70	0.75	2.26

The parameter values for the granite are obtained by averaging the corresponding parameter values; the parameter values for sand are taken as surrogate approximations that are identical to the corresponding parameter values of the granite with similar mineral compositions

6 Parameter sensitivity analyses

While acknowledging the possibility of transient sensitivities of the system's thermal behavior to some parameters, let $T=T(a_1, a_2, \cdots)$ denote the temperature of the outflow water in any of the vertical fractures at steady state, as a function of a set of the major model parameters, $\{a\}=\{a_1, a_2, \cdots\}$, which may include the heat source temperature and initial temperature, apertures of the open vertical fractures, porosities of the sand in the filled vertical fractures, water velocities in the vertical fractures, volumetric specific heat, and thermal conductivity of the rock matrix. Let a_i^* be a base value of parameter a_i and a_i^k be the kth chosen value of a_i where the sensitivity is needed, then at $\{a\}=\{\cdots, a_{i-1}^*, a_i^k, a_{i+1}^*, \cdots\}$, the relative sensitivity coefficient of T with respect to a_i can be expressed as

$$\beta_i^k = \left.\frac{\partial T}{\partial a_i}\frac{a_i}{T}\right|_{\{a\}=\{\cdots, a_{i-1}^*, a_i^k, a_{i+1}^*, \cdots\}}, \quad i = 1, 2, \cdots. \tag{11}$$

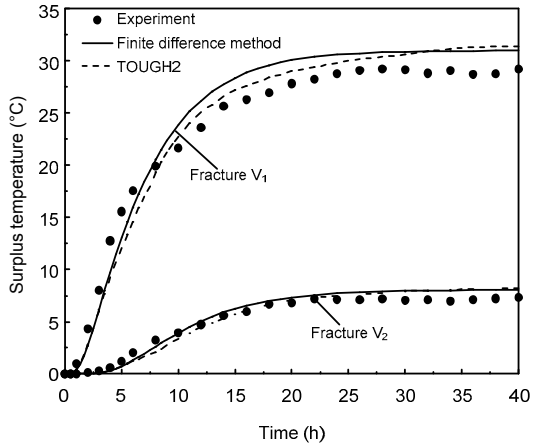

Fig. 6 Temporal variation of temperature of outflow water in open vertical fractures (experiment b)

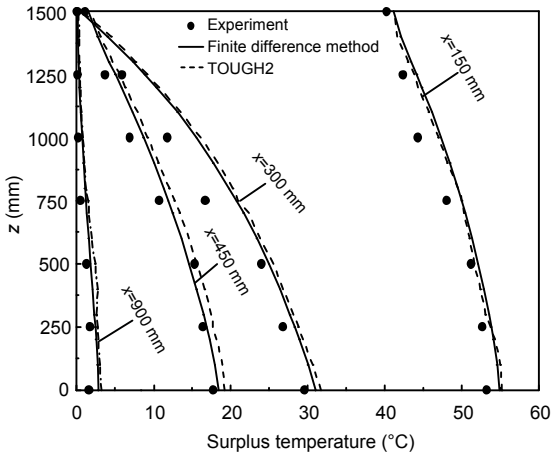

Fig. 7 Steady state distributions of temperature along the height (experiment b)

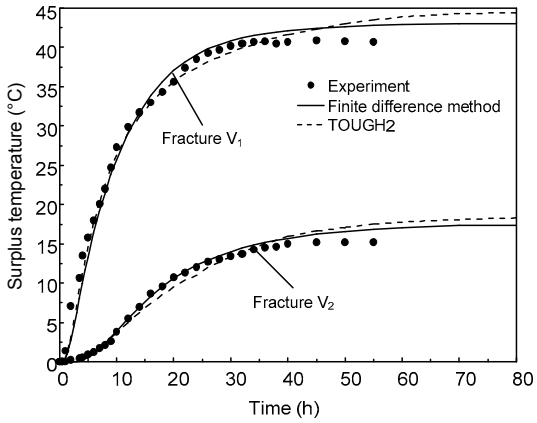

Fig. 8 Temporal variation of temperature of outflow water in filled vertical fractures (experiment e)

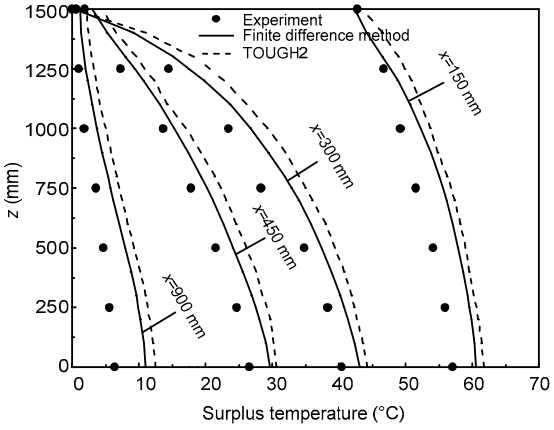

Fig. 9 Steady state distributions of temperature along the height (experiment e)

To evaluate the relative sensitivities numerically, Eq. (11) can be written in a finite difference form:

$$\beta_i^k = \frac{T^{k+} - T^{k-}}{2\Delta a_i^k} \frac{a_i^k}{T^k}, \quad i = 1, 2, \cdots, \tag{12}$$

where T^k, T^{k-}, and T^{k+} stand for the numerically calculated temperature values for $\{a\}$ equating $\{\cdots, a_{i-1}^*, a_i^k, a_{i+1}^*, \cdots\}$, $\{\cdots, a_{i-1}^*, a_i^k - \Delta a_i^k, a_{i+1}^*, \cdots\}$, and $\{\cdots, a_{i-1}^*, a_i^k + \Delta a_i^k, a_{i+1}^*, \cdots\}$, respectively, with Δa_i^k being an increment of a_i^k, usually taken as less than 5% of a_i^k.

Using the parameter values in Tables 2 and 3 for experiment d as the base values of the parameters, a_i^* (i=1, 2, …), the relative sensitivity coefficients of the outflow water temperatures of the vertical fractures with respect to the major model parameters are shown in Fig. 10, in which the parameter stands for the heat source temperature T_h, the initial rock model temperature T_0, the vertical fracture V_1 water velocity v_1, the vertical fracture V_2 water velocity v_2, the volumetric specific heat of the rock matrix $\rho_r c_r$, and the thermal conductivity of the rock matrix K_r, respectively. According to Table 4, the degrees of relative parameter sensitivities can be categorized into four different classes based on the range of values of the relative sensitivity coefficients, and the classes of parameter sensitivities for the outflow water temperatures of the vertical fractures are given in Table 5. Note that the temperature of water in fracture V_2 is highly sensitive to the velocity of water in fracture V_1, whereas the temperature of water in

fracture V_1 is rather insensitive to the velocity of water in fracture V_2. The relative sensitivities to the apertures of the fractures and the porosities of sand in the filled fractures, which are not shown, are the same as the relative sensitivities to the relevant water velocities.

7 Conclusions

Water flow and heat transfer experiments and numerical calculations were conducted for a meter-scale rock model composed of granite blocks with two horizontal fractures and two vertical fractures of pre-set apertures under open or sand-filled conditions.

The experiments indicated that the heat advection due to water flow in the vertical fracture nearest to the heat source played a major role in influencing the spatial distributions and temporal variations of the temperature, through carrying the input thermal energy out of the model and impeding heat conduction in the transverse direction, and such effects increased with larger water fluxes in the fractures and decreased with higher heat source temperature and/or larger distance of the fracture from the heat source. Enhanced heat conduction was observed when the fractures were filled with sand, and transverse heat transfer became more pronounced than the cases with open fractures. Water in the two horizontal fractures essentially remained standstill and played a role of enhancing heat storage and conduction. There was no phase change of the water in the fractures, which was

Table 4 Classification of relative parameter sensitivities (Lenhart *et al*., 2002)

Class	Index	Sensitivity
I	$0 < \lvert \beta_i^k \rvert < 0.05$	Small to negligible
II	$0.05 \leq \lvert \beta_i^k \rvert < 0.2$	Medium
III	$0.2 \leq \lvert \beta_i^k \rvert < 1$	High
IV	$1 \leq \lvert \beta_i^k \rvert$	Very high

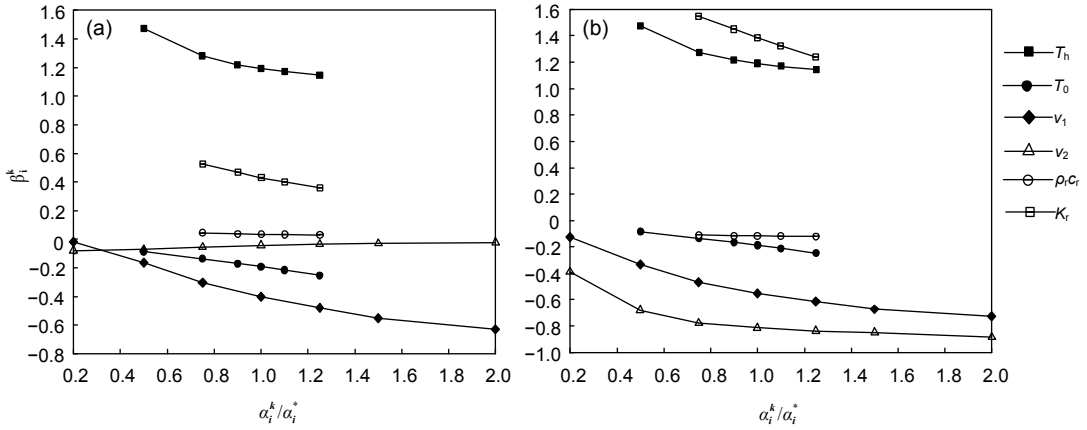

Fig. 10 Relative sensitivity β_i^k of the outflow water temperatures of vertical fractures V_1 (a) and V_2 (b) with respect to parameter α_i^k with α_i^* being the base value

Table 5 Classes of parameter sensitivities for the outflow water temperatures of the vertical fractures

Parameter	Index		Class	
	Fracture V_1	Fracture V_2	Fracture V_1	Fracture V_2
Water velocity in fracture V_1	−0.64—−0.03	−0.73—−0.13	From I to III when the parameter increases	From II to III when the parameter increases
Water velocity in fracture V_2	−0.09—−0.03	−0.89—−0.39	From I to II when the parameter increases	III
Heat source temperature	1.15–1.46	1.14–1.48	IV	IV
Initial temperature	−0.25—−0.09	−0.25—−0.09	From II to III when the parameter increases	From II to III when the parameter increases
Volume specific heat of rock	0.02–0.04	0.01–0.02	I	I
Thermal conductivity of rock	0.35–0.52	1.26–1.55	III	IV

mainly due to the experimental arrangement of no direct exposure of the fractured rock model to the atmosphere, and the hydraulic head at steady state assumed nearly linear distribution along the vertical fractures.

The numerical scheme was formulated and coded by using finite difference for the model domain and the fourth order Runge-Kutta method for the resulting 1st order ordinary differential equations with respect to time. In general, good consistency was observed for comparisons of the numerical calculations using both the developed code and the TOUGH2 software with the experimental data, and it was found that the effects due to a certain degree of unavoidable heat loss during the experiments, albeit relatively minor in general, could get more pronounced at locations where the temperatures were significantly lower than the heat source temperature.

Relative sensitivities of the temperature of the outflow water in the vertical fractures with respect to a set of major model parameters were calculated, which revealed that, in addition to the heat source temperature and the thermal conductivity of the rock matrix, the velocity of water in the fracture nearest to the heat source, when increased, changed from being an insensitive parameter into acting as a highly sensitive parameter.

References

Alonso, E.E., Alcoverro, J., Coste, F., Malinsky, L., Merrien-Soukatchoff, V., Kadiri, I., Nowak, T., Shao, H., Nguyen, T.S., Selvadurai, A.P.S., *et al*., 2005. The FEBEX benchmark test: case definition and comparison of modelling approaches. *International Journal of Rock Mechanics and Mining Sciences*, **42**(5-6):611-638. [doi:10.1016/j.ijrmms.2005.03.004]

Čermak, V., Jetel, J., 1985. Heat flow and ground water movement in the Bohemian cretaceous basin (Czechoslovakia). *Journal of Geodynamics*, **4**(1-4):285-303. [doi:10.1016/0264-3707(85)90065-1]

Chan, T., Khair, K., Jing, L., Ahola, A., Noorishad, M., Vuillod, E., 1995. International comparison of coupled thermo-hydro-mechanical models of a multiple-fracture bench mark problem: DECOVALEX phase I, bench mark test 2. *International Journal of Rock Mechanics and Mining Sciences*, **32**(5):435-452. [doi:10.1016/0148-9062(95)00034-E]

Cheng, A.H.D., Ghassemi, A., Detournay, E., 2001. Integral equation solution of heat extraction from a fracture in hot dry rock. *International Journal for Numerical and Analytical Methods in Geomechanics*, **25**(13):1327-1338. [doi:10.1002/nag.182]

Chijimatsu, M., Fujita, T., Sugita, Y., Amemiya, K., Kobayashi, A., 2001. Field experiment, results and THM behaviour in the Kamaishi mine experiment. *International Journal of Rock Mechanics and Mining Sciences*, **38**(1):67-68. [doi:10.1016/S1365-1609(00)00065-4]

Ghassemi, A., Tarasovs, S., Cheng, A.H.D., 2003. An integral equation solution for three-dimensional heat extraction from planar fracture in hot dry rock. *International Journal for Numerical and Analytical Methods in Geomechanics*, **27**(12):989-1004. [doi:10.1002/nag.308]

Gringarten, A.C., Witherspoon, P.A., Ohnishi, Y., 1975. Theory of heat extraction from fractured hot dry rock. *Journal of Geophysical Research*, **80**(8):1120-1124. [doi:10.1029/JB080i008p01120]

Ito, A., Yum, M., Sugita, Y., Kawakami, S., 2004. A Research Program for Numerical Experiments on the Coupled Thermo-Hydro-Mechanical and Chemical Processes in the Near-Field of a High-Level Radioactive Waste Repository. *In*: Stephansson, O. (Ed.), Coupled Thermo-Hydro-Mechanical-Chemical Processes in Geo-Systems: Fundamentals, Modelling, Experiments and Applications, **2**:353-358. [doi:10.1016/S1571-9960(04)80066-1]

Jing, L., Tsang, C.F., Stephansson, O., 1995. DECOVALEX—an international co-operative research project on mathematical models of coupled THM processes for safety analysis of radioactive waste repositories. *International Journal of Rock Mechanics and Mining Sciences & Geomechanics Abstracts*, **32**(5):389-398. [doi:10.1016/0148-9062(95)00031-B]

Lenhart, T., Eckhardt, K., Fohrer, N., Frede, H.G., 2002. Comparison of two different approaches of sensitivity analysis. *Physics and Chemistry of the Earth, Parts A/B/C*, **27**(9-10):645-654. [doi:10.1016/S1474-7065(02)00049-9]

Liu, Q., Zhang, C., Liu, X., 2006. Numerical modeling and simulation of coupled THM processes in Task-D of DECOVALEX IV. *Chinese Journal of Rock and Mechanics and Engineering*, **25**(4):709-720 (in Chinese).

Liu, X., Xiang, Y.Y., 2012. Numerical modeling of water flow and heat transfer in a meter-scale physical model of fractured rocks. *Rock and Soil Mechanics*, **33**(1):287-294 (in Chinese).

Millard, A., Stietel, A., Bougnoux, A., Vuillod, E., 1996. Generic Study of Coupled THM Processes of Nuclear Waste Repositories as Far-Field Initial Boundary Value Problems (BMT1). *In*: Stephansson, O., Jing, L., Tsang, C.F. (Eds.), Coupled Thermo-Hydro-Mechanical Processes of Fractured Media: Mathematical and Experimental Studies, **79**:245-279. [doi:10.1016/S0165-1250(96)80029-0]

Rutqvist, J., Borgesson, L., Chijimatsu, M., Nguyen, S.T., Jing, L., Noorishad, J., 2001. Coupled thermo-hydro-mechanical analysis of a heater test in fractured rock and bentonite at Kamaishi Mine—comparison of field results to predictions of four finite element codes. *International Journal of Rock Mechanics and Mining Sciences*, **38**(1):129-142. [doi:10.1016/S1365-1609(00)00069-1]

Rutqvist, J., Chijimatsu, M., Jing, L., Millard, A., Nguyen, T.S., Rejeb, A., 2005. Numerical study of the THM effects on the near-field safety of a hypothetical nuclear waste repository-BMT1 of the DECOVALEX III project. Part 3: Effect of THM coupling in sparsely fractured rocks. *International Journal of Rock Mechanics and Mining Sciences*, **42**(5-6):745-755. [doi:10.1016/j.ijrmms.2005.03.012]

Schulz, R., 1987. Analytical model calculations for heat exchange in a confined aquifer. *Journal of Geophysics*, **61**:12-20.

Tao, W., 2003. Numerical Heat Transfer (2nd Edition). Xi'An Jiaotong University Press, China (in Chinese).

Tsang, C.F., Jing, L., Stephansson, O., Kautsky, F., 2005. The DECOVALEX III project: a summary of activities and lessons learned. *International Journal of Rock Mechanics and Mining Sciences*, **42**(5-6):593-610. [doi:10.1016/j.ijrmms.2005.03.003]

Tsang, C.F., Stephansson, O., Jing, L., Kautsky, F., 2009. DECOVALEX project: from 1992 to 2007. *Environmental Geology*, **57**(6):1221-1237.

Wilcock, P., 1996. Generic Study of Coupled T-H-M Processes in the Near Field (BMT3). *In*: Stephansson, O., Jing, L., Tsang, C.F. (Eds.), Coupled Thermo-Hydro-Mechanical Processes of Fractured Media: Mathematical and Experimental Studies, **79**:311-340. [doi:10.1016/S0165-1250(96)80031-9]

Xiang, Y.Y., Guo, J.Q., 2011. A Laplace transform and Green function method for calculation of water flow and heat transfer in fractured rocks. *Rock and Soil Mechanics*, **32**(2):333-340 (in Chinese).

Xiang, Y.Y., Zhang, Y., 2012. Two-dimensional integral equation solution of advective-conductive heat transfer in sparsely fractured water-saturated rocks with heat source. *International Journal of Geomechanics*, **12**(2):168-175. [doi:10.1061/(ASCE)GM.1943-5622.0000109]